Comparison of external bulk video imaging with focused beam reflectance measurement and ultra violet-visible spectroscopy for metastable zone identification in food and pharmaceutical crystallization processes

Levente L. Simon[1‡], *Zoltan K. Nagy*[2#], *Konrad Hungerbuhler*[‡]

[‡]ETH Zurich, Institute of Chemical and Bioengineering, Switzerland

[#]Loughborough University, Chemical Engineering Department, Loughborough, LE11 3TU, United Kingdom

Abstract

The purpose of the paper is twofold: it describes the proof of concept of the newly introduced bulk video imaging (BVI) method and it presents the comparison with existing process analytical technologies (PAT) such as focused beam reflectance measurement (FBRM) and ultra violet/visible (UV/Vis) spectroscopy. While the latter two sample the system in small volumes closely to the probe, the BVI approach monitors the entire or large parts of the crystallizer volume. The BVI method is proposed as a complementary noninvasive PAT tool and it is shown that it is able to detect the boundaries of the metastable zone with comparable or better performance than the FBRM and UV/VIS probes.

[1] On research stay at the Loughborough University, U.K.
[2] Corresponding author. Tel: +44 (0)1509 222516. E-mail address: z.k.nagy@lboro.ac.uk.

1. Introduction

Metastable zone identification is the first step during the design of crystallization systems required to ensure reproducible crystal characteristics. Since the metastable zone width (MSZW) is not a thermodynamic property it changes in function of several system characteristics such as: cooling rate, degree of stirring, solution history and presence of foreign particles (impurities or additives). The accurate determination of the metastable zone allows improved supersaturation control policies, it helps to avoid secondary nucleation, ensures maximal productivity and the desired particle size distribution (PSD) at the end of the batch (Braatz, 2002, Nagy et al., 2008).

The experimental determination of the MSZW is usually performed by increasing the supercooling at a constant rate until the formation of detectable particles (apparent nucleation) is observed, and by heating the suspension at a constant rate until the disappearance of particles (apparent solubility) is detected. The term 'nucleation' often used in the definition of the MSZ usually indicates the formation of particles of detectable number and size, which usually implies the formation of the critical cluster (as indicated by the classical nucleation theory) and growth of the particles to the detectable size. Generally the goal is to detect the formation of particles as close as possible to the actual nucleation (formation of critical cluster). In order to determine the MSZW several sensors can be considered: turbidity (Parsons et al., 2003), focused beam reflectance measurement (Fujiwara et al., 2002, O'Grady et al., 2007), spectroscopy (Fujiwara et al., 2002, O'Grady et al., 2007, Pollanen et al., 2006), ultrasonic velocity measurements (Gurbuz and Ozdemir, 2003), density (Marciniak, 2002a) and electrical conductivity monitoring (Lyczko et al., 2002), hot stage microscopy (Kumar et al., 1996), quartz crystal based monitoring (Joung et al., 2005, Loffelmann and Mersmann, 2002), and last but not least by visual inspection of the crystallizer content (Sohnel and Mullin, 1988). The detection of the first nucleation events is a function of the used sensor, e.g. Fujiwara et al. (2002) concluded that for the paracetamol system the FBRM provided the highest sensitivity towards nucleation detection, followed by the attenuated total reflection (ATR) – Fourier transform infrared (FTIR) spectroscopy and visual inspection.

Marciniak (2002b) compared the density, ultrasonic velocity and transparency signals for the MSZW identification of the fluoranthene in trichloroethylene (Marciniak, 2002b). The author concluded that the solution transparency was the most sensitive method, whereas De Anda et al., (2005) observed that the fiber optic turbidity probe shows a time lag in detecting the nucleation onset.

Some of the measurement techniques detect the nucleation event directly by sensing the newly formed nuclei, e.g. FBRM and in-process video microscopy (PVM) systems. The requirement of these probes is that the particle has to be large enough to be detectable (usually above approximately 1 micron) and it has to pass through a small detection volume. The probability that the first nucleus passes the detection volume decreases as the crystallizer volume increases. Furthermore, it is well known that a certain solid concentration in the liquid is needed to obtain a statistically representative FBRM signal. The advantage of the FBRM and PVM type sensors for nucleation onset monitoring is that these measure nucleation events (formation of new particles) and not the property of the bulk solution. The second class of measurement devices (spectroscopy, conductivity) monitors the change of the crystallizer liquid phase characteristics (absorbance, conductivity, density) during the nucleation. Since these measure the bulk properties, a reasonable amount of property change is needed in order to show the nucleation events. In this article the bulk video imaging method (BVI) is compared with FBRM and UV/Vis spectroscopy for metastable zone identification and the detection of the onset of the apparent nucleation. The particular feature of the BVI method is that it monitors the formation/dissolution of the solid phase but using information from the bulk suspension, providing a noninvasive, low-cost, automated method for MSZW determination, making it a well-suited methodology in the pharmaceutical and food industries. The methods are corroborated for the batch cooling suspension crystallization of the model pharmaceutical compound caffeine, and in the case of the crystallization from melt of palm oil, an important product of the food industries. According to the authors' knowledge this is the first time when the application of PAT tools are evaluated for highly viscous crystallization systems from melt, often applied in the food industries.

The article is structured as follows: after the description of the BVI method in the second section, the third section describes the experimental setup and materials, followed by the presentation of the comparison results before the final conclusions are drawn.

2. The bulk video imaging method (BVI)

The BVI method is based on a video capture hardware, which captures several pictures of the crystallization bulk per second. The video camera is placed externally and the crystallizer vessel is covered with black folia in order to ensure a dark background, in the case of glass crystallization system. For larger scale applications the camera can be used through an observation window or a process endoscope can be employed. After the frames are transferred to the personal computer, the image processing algorithm cuts out the interrogation window from the current frame, converts the image to the grey (8 bit) format and it calculates the mean grey intensity (MGI) index. The flowchart of the BVI method is shown schematically in Figure 1.

Such an image is a two dimensional matrix (width × length) which contains grey intensity values ranging from 0 to 255 (0 corresponds to 100% black and 255 to 100% white). The next step is the calculation of the MGI index:

$$MGI = \frac{\sum_{i=0}^{N} PGI_i}{N} \tag{1}$$

where PGI_i is the pixel grey intensity of each pixel i and N is the total number of pixels in the picture. The BVI using the average intensity value provides a robust, straightforward, real-time feasible and adjustment free strategy to monitor the nucleation onset. During the on-line monitoring of the crystallization process the MGI value is compared to a previously set MGI threshold value. This threshold value is selected in function of the noise in the MGI values. In case the noise is significant a moving average filter may be applied to the video data and the signal is smoothed out. However, a

detection delay is inherently introduced depending on the size of the filter window. Once the threshold MGI value has been exceeded it is concluded that the nucleation onset has occured.

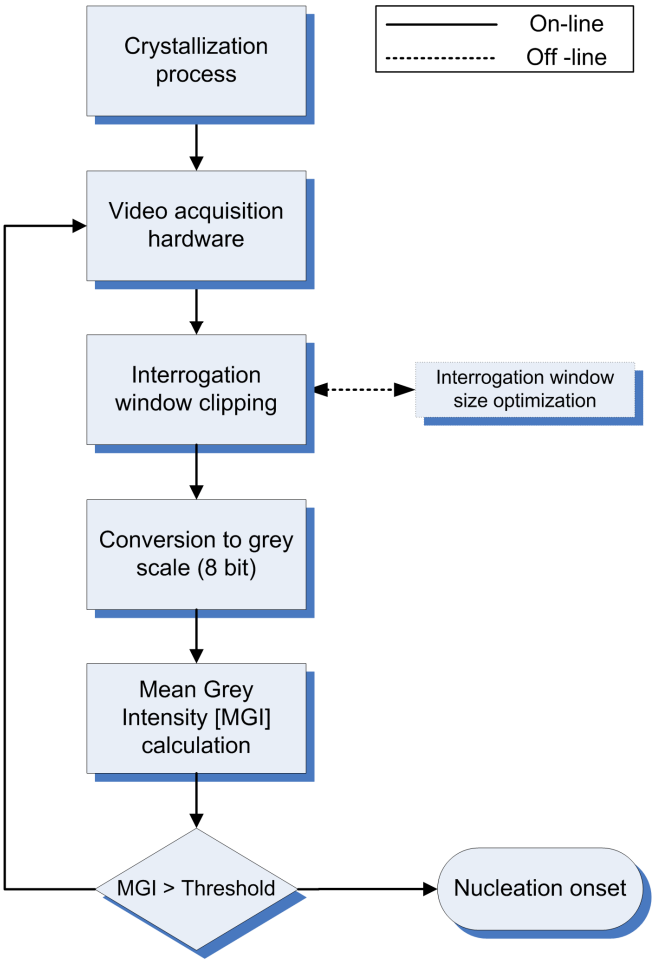

Figure 1. Information flow during crystallization bulk video imaging (BVI).

Interrogation window optimization

After the first crystallization batch has been completed there is sufficient video information to optimize off-line the size of the interrogation window. This is required to find a compromise between the noise in the MGI trend and the influence on the mean grey value. If the interrogation window is large the particle will pass through it with high probability thus it can be detected. However, the impact on the MGI value is low since the ratio of the particle size to the interrogation window is low. In contrast to this, if the

interrogation window is small the particle passing through it will cause a significant increase in the MGI value, thus it is detected early. The optimal interrogation window size also depends on the algorithm used to detect the crystallization onset. Small windows will detect the particles faster however the signal will appear as noisy, thus if a threshold value of the MGI is used this may lead to detection problems.

3. Materials and equipment

Anhydrous caffeine from Sigma-Aldrich with a minimum purity of 98% and deionised water were used in all experiments related to the caffeine investigation. Refined, bleached and deodorised (RBD) palm oil was supplied by Golden Jomalina Sdn. Bhd. (Sepang, Malaysia) and shipped from the Malaysian Palm Oil Board (MPOB). In all cases the crystallizer content was heated above the saturation/melting temperature and kept for 30 minutes. The process analytical technology used consists of the FBRM and ATR-UV/VIS probes, which were used to simultaneously monitor the system. The bulk phase of the crystallizer is monitored using a Sony video camera which captures 25 frames/second. The video signal is compressed using a Pinnacle TV capture card with hardware encoding capabilities.

A D600l-HC-K Lasentec FBRM probe (Mettler-Toledo Autochem Ltd, Leicester, UK) was used and data were collected every 10s in the 1-1000 μm, 90 log channels mode. The liquid phase is monitored using a Zeiss MCS 500 spectrometer with a Hellma 661.812 Attenuated Total Reflection (ATR) UV/Vis probe (supplied by Clairet Scientific, Northampton, UK). Due to the existence of chromophoric group in the caffeine molecule the compound absorbs UV light. The UV spectra of caffeine has two characteristic peaks at 205 and 274 nm and the absorbance at these wavelengths can be used to monitor the concentration change in the solution during the crystallization. The temperature was maintained using a Huber Ministat unit (Radleys Ltd, Saffron Waldon, Essex, UK), which was controlled with a PC using a software written in Labview (National Instruments, US). Agitation was held constant at 200 rpm by a Heidolph RZR2021 motor

(Heidolph Instruments GmbH & Co. KG, Schwabach, Germany). The experimental setup and the process analytical equipment are presented in Figure 2.

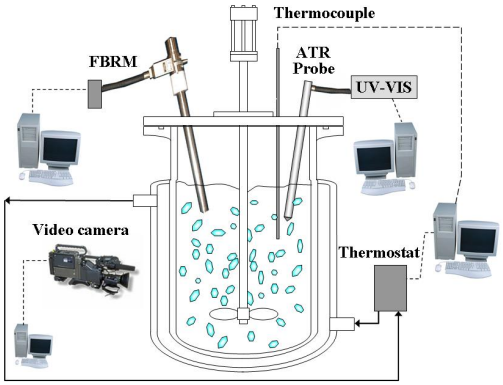

Figure 2. Schematic representation of the experimental equipment.

4. Results and discussion.

In order to determine the caffeine metastable zone several experiments were performed with 0.3 °C/min and 0.7 °C/min cooling ramps at several concentrations as shown in Table 1. The nucleation onset during the palm oil melt crystallization was monitored during cooling with 0.67 °C/min and 2 °C/min rates.

Table 1 List of experiments.

Exp. No.	Compound	Cooling rate [°C/min]	Concentration [g/g water]	Captured image size [pixel × pixel]	Processed image size [pixel × pixel]
1	Caffeine	0.3	0.05	720 × 576	335 × 245
2	Caffeine	0.7	0.05	720 × 576	300 × 306
3	Caffeine	0.7	0.065	352 × 576	135 × 385
4	Caffeine	0.7	0.08	352 × 576	135 × 385
5	Palm oil	0.67	-	352 × 576	135 × 385
6	Palm oil	2	-	352 × 576	135 × 385

In order to compare the FBRM signal with the MGI index, throughout this work, two count ranges were used: 1-5.012 and 1-1000 micron. The MGI index trend is calculated for the region of interests specified in Table 1. In all cases, nucleation onset was considered when the FBRM, BVI or UV/Vis signal has changed more then 5% compared to the moving average value calculated on a 3 minutes window. The monitoring results obtained for the first experiment with the cooling rate 0.3 °C/min are shown in Figure 3.

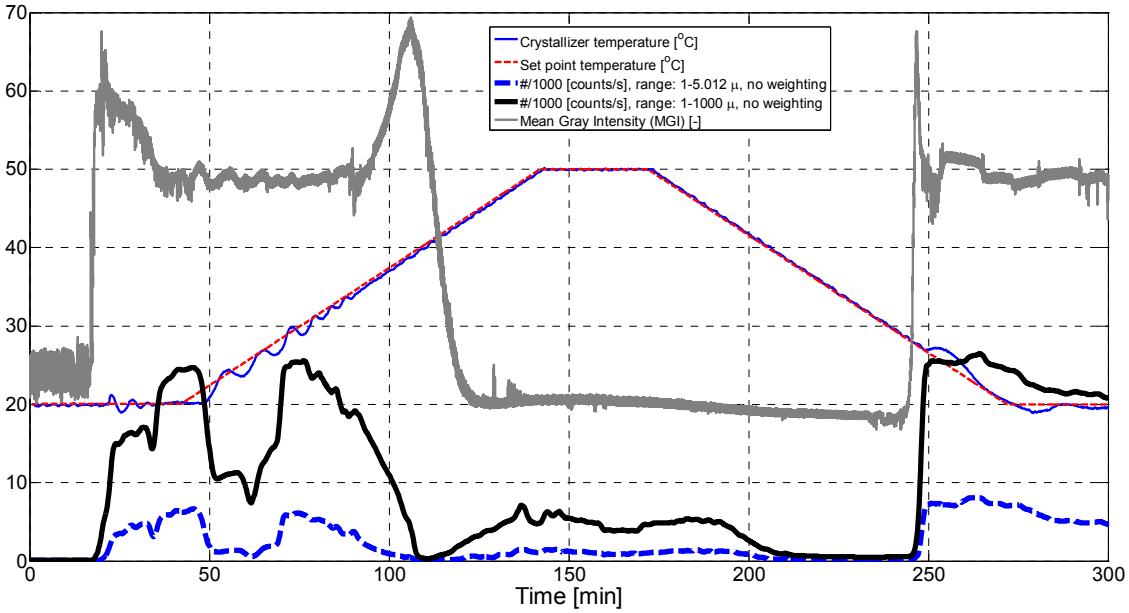

Figure 3. Comparison of the BVI and FBRM data for the caffeine crystallization, 0.3 °C/min cooling rate, experiment 1.

The experiment was started by adding water in the crystallizer and since the crystallizer unit was covered with a black material, the grey mean intensity of the initial pictures is low, showing a dark image. After the caffeine anhydrate was added, which has white color, the MGI value has increased. The feeding event can be clearly observed in the BVI and FBRM data, and slightly in the temperature signal. The solution was heated up and kept at 50 °C for 30 min after which the cooling ramp is started. The increase in the FBRM counts after the dissolution of caffeine at about 120 min is due to the formation of bubbles due to the dissolved air in the water. In this experiment the water was not degassed and as the temperature increased water bubbles formed in the liquid and on the FBRM probe window. After the bubbles were eliminated and the temperature decreased

at about 200 min, the FBRM signal decreased close to the original baseline value. A slight decrease in the MGI trend can also be observed after 170 min as the bubbles are removed from the solution. Since bubbles are less dark than the crystallizer background, the MGI value is higher while they are present, and as they are removed the MGI value decreases. The nucleation of the hydrated caffeine is signaled by the sharp increase of the MGI value and the FBRM counts around 240 min. In this case similar detection performances are observed for both the FBRM and BVI methods.

The shape of the BVI signal can be explained by the changes in flowability properties of the suspension, due to the polymorphic transformations between the hydrate and anhydrous forms occurring during the crystallization process. Since the two forms have very different morphologies (see Figure 4) the mixing conditions and overall visual aspect of the suspension change after the transformation.

a) b)

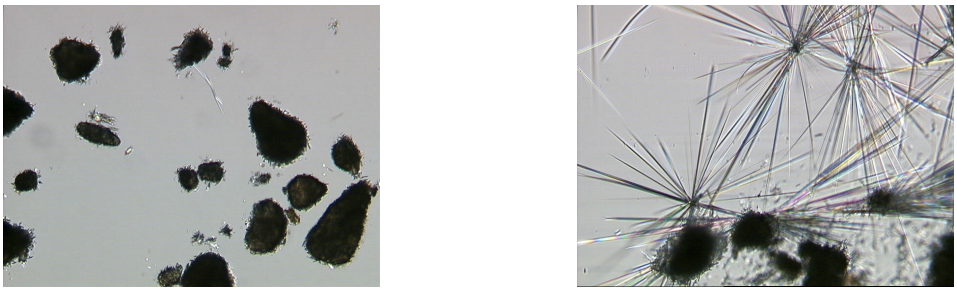

Figure 4. Micrographs showing the (a) particles of anhydrous caffeine and (b) the mixture of anhydrous caffeine particles together with the hydrates with needle morphology.

After the caffeine anhydrate is charged the MGI increases to 60-65 units after which, during transformation to the hydrate, drops to around 50. After the heating ramp is started the hydrate is converted back to the anhydrate which is the more stable form at higher temperatures. Bothe and Cammenga (Bothe and Cammenga, 1980) reported that the hydrate form can be obtained when the crystallization is started below 40 °C, however this value is a function of the cooling rate as it is shown later. The MGI value starts to increase when the temperature approaches 38 °C and the MGI eventually reaches the value of 70. This event is explained by the fact that the hydrate has converted to the

anhydrous form, having the same MGI value as the addition of the raw material (anhydrate). After this event the solid anhydrate is dissolved in water and the MGI value drops to a steady value. Upon the nucleation onset it is observed that the MGI value increases sharply to 70 and drops to 50, value which was recorded earlier during the hydratation process. Note that the apparent nucleation (nucleation followed by growth) is also indicated by the change in the temperature of the system at about 250 min, when the sudden heat generated by the nucleation and immediately following growth induces a disturbance in the temperature control system. Figure 3 indicates that the detectable temperature change occurs delayed compared to the FBRM signal. If more advanced calorimetric systems are used it is expected that this delay would be reduced, however it is likely that the calorimetric method generally would be slower to indicate nucleation than the BVI. Using a small-scale reaction calorimeter CRC.v4 (Billeter et al., 2008), which implements the principle of power compensation via an electrical heater, apparent nucleation can be detected more accurately.

The data for the second experiment (0.7 °C/min cooling) is shown in Figure 5 and Figure 6 (zoomed). Similarly to the previous experiment, the BVI is able to detect the onset of the apparent nucleation with comparable performance to the FBRM probe. The MGI trend shows similar features to the previous experiment. Note that the formation of bubbles is not a problem here since the same solution was used as in experiment 1 hence bubbles were removed during the previous experiment heating/cooling process. These results illustrate the advantage of the BVI method compared to the FBRM in showing lower sensitivity to the existence of bubbles in the solution. The baseline in the case of the BVI measurement is very similar for both experiments (experiments 1 and 2), with a small drift only indicating the presence/removal of bubbles, whereas the FBRM shows significant change in the number of counts/s due to the presence of bubbles, which in some cases can be at the level which may yield misinterpretation of the data by considering false nucleation events.

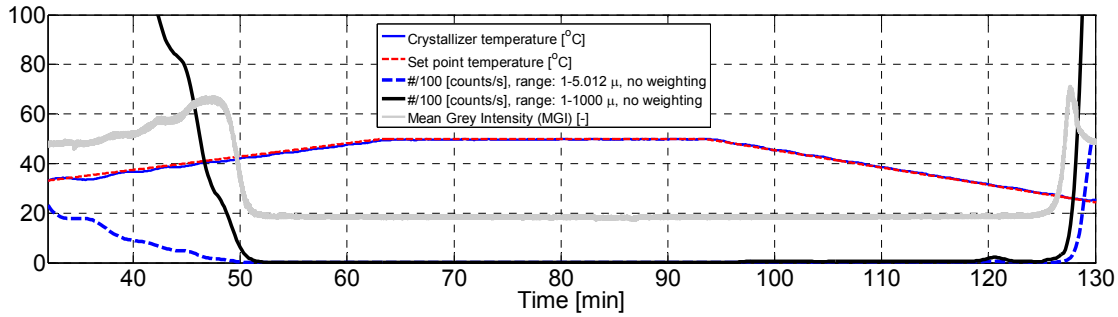

Figure 5. Comparison of the BVI and FBRM data for the caffeine crystallization, 0.7 °C/min cooling rate, experiment 2.

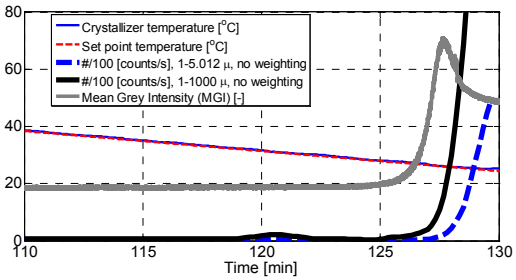

Figure 6. Zoomed comparison of the BVI and FBRM data for the caffeine crystallization, 0.3 °C/min cooling rate, experiment 2.

The caffeine crystallization progress is shown in Figure 7 at several time instances.

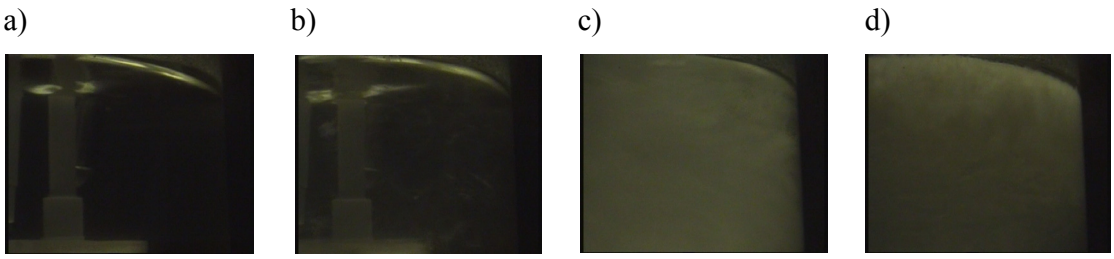

Figure 7. Bulk video images during caffeine crystallization (0.7 °C/min cooling rate, experiment 2) at different time instances: a) 120 min, b) 126.5 min, c) 127.5 min, d) 130 min.

In the third and fourth experiments the BVI method is compared to the UV/Vis spectroscopy signal, as shown in Figure 8 and Figure 9. The BVI signal presents the same trend as previously observed. The UV/Vis data shows a peak around the same time instance. During nucleation the absorbance should decrease since the solute concentration

decreases. However a common phenomenon observed using ATR probes for crystallization monitoring is that for many systems the nucleation tends to happen on the surface of the probe. This leads to an increase in the molar absorptivities at all wave lengths and an increase in the absorbance values. Additionally, since both the FBRM and the ATR-UV/Vis (or ATR-FTIR) are invasive probes they may act as initiators for nucleation, which for many systems results in particles adhering to the surface of the probe compromising the measurement. The BVI method can be used as an external noninvasive monitoring approach eliminating the aforementioned problems related to the FBRM and ATR spectroscopy.

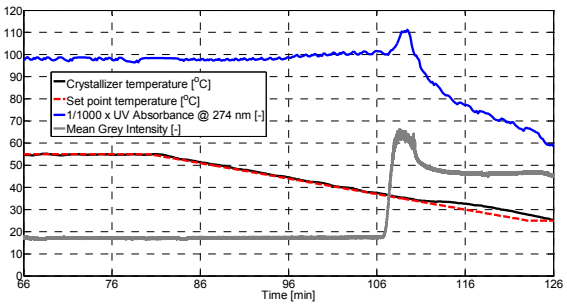

Figure 8. Comparison of the BVI and UV/Vis spectroscopy data for the caffeine crystallization, 0.3 °C/min cooling rate, experiment 3.

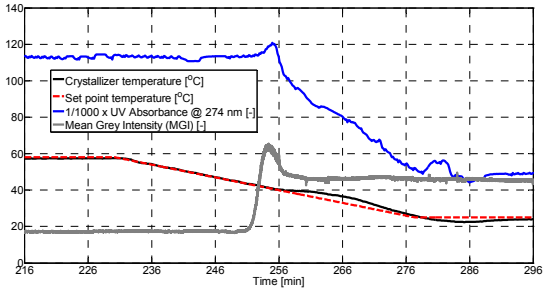

Figure 9. Comparison of the BVI and UV/Vis spectroscopy data for the caffeine crystallization, 0.3 °C/min cooling rate, experiment 4.

The identified caffeine metastable zone is shown in Figure 10 where the solubility curve is calculated according to the van't Hoff correlation with the parameters identified by Nagy et al., (2007). Additional experimental solubility data points reported by Bustamante et al., (2002) are also presented.

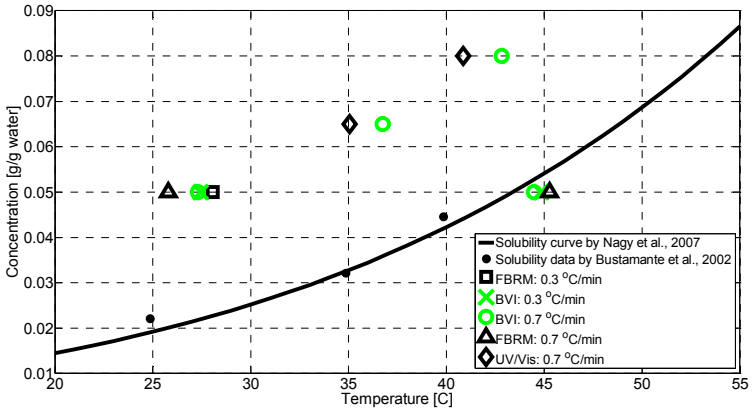

Figure 10. Caffeine metastable zone width identification using the BVI, FBRM, UV/Vis signals and the corresponding cooling rates. Solubility curve is expressed in terms of the anhydrous caffeine.

In this figure it is observed that the BVI method identifies a narrower metastable zone indicating that this method detects earlier the formation of particles.

The BVI method was corroborated in the case of the crystallization of palm oil from melt using two different cooling rates. The palm oil was heated and kept at 70 °C for 30 min to make sure that it is completely melted. The experimental results using a cooling rate of 0.67 °C/min are presented in Figure 11. The results show that the nucleation onset was detected approximately 3 min sooner by the BVI approach compared to the FBRM probe. The same conclusions are drawn from the experiment number 6 when a higher cooling rate of 2 °C/min was used. Figure 12 indicates that using the higher cooling rate the BVI method detects the nucleation with 15 minutes sooner than the FBRM. The results were in correlation with visual observation which also indicated the cloudiness of the suspension much earlier before any change in the FBRM signal was detected.
The images showing the progress of crystallization of the palm oil from melt are shown in Figure 13 and Figure 14 at several time instances.
The large difference between the induction time detected by the BVI and FBRM methods is due to the fact that during the fast cooling of palm oil a large number of small crystals form, which are below the detection limit of the FBRM. These small particles are very large in number and provide a cloud formation in the bulk which can be detected by the BVI. Despite the visually observable cloudiness of the solution, the FBRM only detects nucleation after the large number of particles grew to the detectable size, about 0.5-1

micron. The faster the cooling rate is, the smaller the crystals forming at nucleation are, and the larger the delay between the moment when BVI and FBRM detect the nucleation events is. At about 205 min after the start of the experiment, the crystals are already present in the solution and detected by the BVI method, Figure 14d.

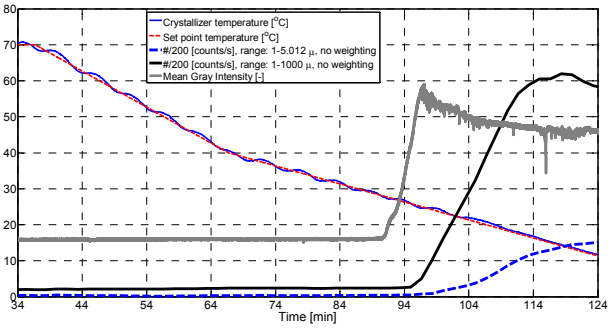

Figure 11. Comparison of the BVI and FBRM data for the palm oil crystallization, 0.67 °C/min cooling rate, experiment 5.

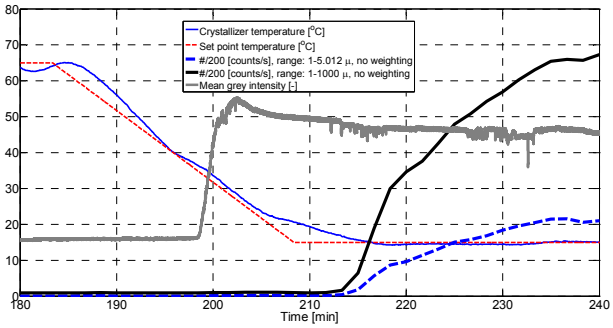

Figure 12. Comparison of the BVI and FBRM data for the palm oil crystallization, 2 °C/min cooling rate, experiment 6.

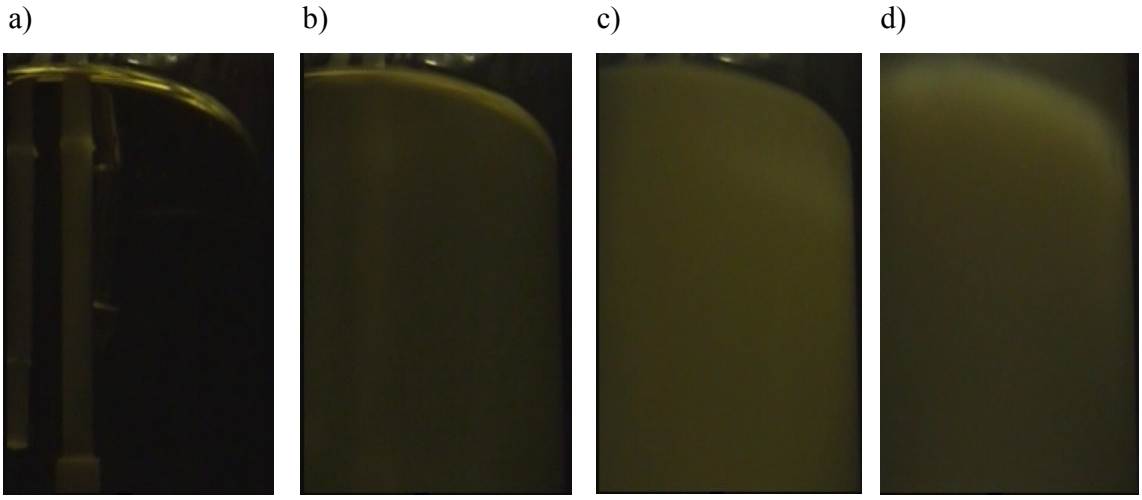

Figure 13. Bulk video images during palm oil crystallization (0.67 °C/min cooling rate, experiment 5) at different time instances: a) 84 min, b) 94 min, c) 96 min, d) 124 min.

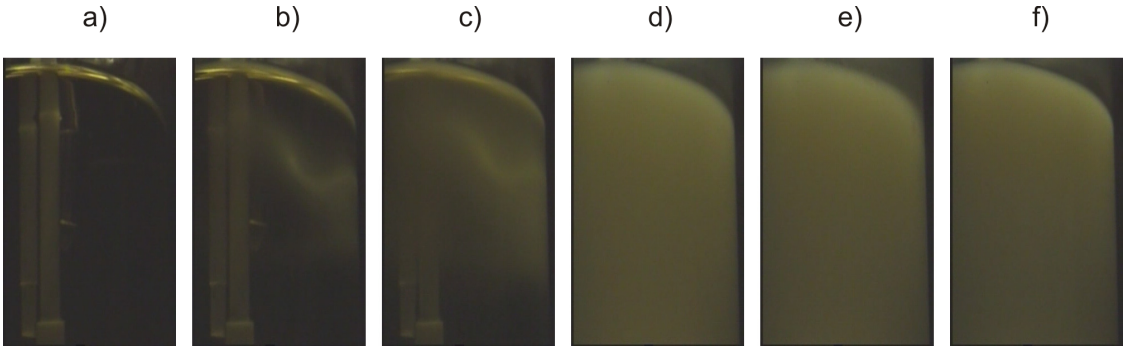

Figure 14. Bulk video images during palm oil crystallization (2 °C/min cooling rate, experiment 6) at different time instances: a) 195 min, b) 199 min, c) 199.5 min, d) 205 min, e) 210 min, f) 220 min.

One of the main advantages of the BVI approach is that it is a non-invasive monitoring solution and it can be installed externally so that measurements are made through the observation window. Hence there are no contamination issues, which can be important in the food and pharmaceutical industries. Also being a bulk monitoring device it shows significantly lower sensitivity to the mixing conditions. The palm oil system for example becomes highly viscous shortly after nucleation, when measurements from FBRM are not reliable anymore, since it is not guaranteed that a representative sample reaches the measurement volume of the probe.

In comparison to in-situ video microscopy (Qu et al., 2006; Kempkes et al., 2008; Li et al., 2008), external on-line imaging (Calderon De Anda et al., 2005; Larsen et al., 2007) and flow-through cell based imaging techniques (Eggers et al., 2009) the BVI may not be suited to monitor particle size characteristics accurately as the image resolution is low and the depth of field is large. This latter aspect makes difficult the calibration of the number of pixels associated to a certain particle size (as the determined particle size is influenced by the distance from the imaging device), however the methodology provides a low-cost and robust metastable zone determination approach.

The influence of the interrogation windows size (Figure 15) on the MGI index is shown in Figure 16, while Figure 17 shows the crystal detected using the MGI trends. By this analysis, it is shown that large interrogation windows filter out the presence of the particles thus are less sensitive. The smaller the window the larger is the detection sensitivity. It is recommended that the window size is chosen in function of the detection algorithm e.g. detection of the crystal appearance event based on peak monitoring or detection of the point where the time-averaged MGI value is above a threshold.

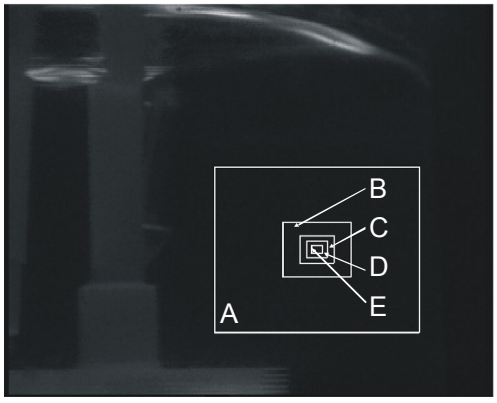

Figure 15. The interrogation windows used in the BVI method.

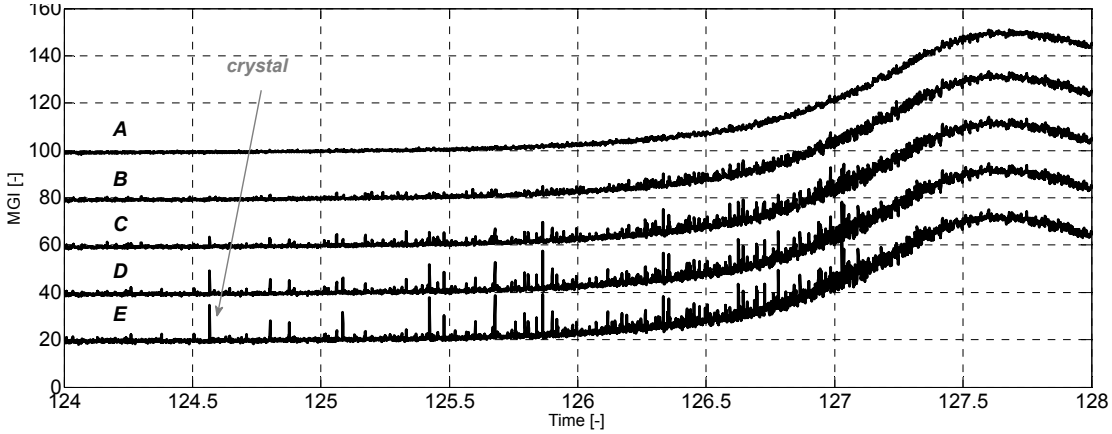

Figure 16. The influence of the interrogation windows size on the MGI index (experiment 2); A: 72900 pixels, B: 8000 pixels, C: 2000 pixels, D: 720 pixels, E: 192 pixels. The E trend has the true MGI [-] value, the other trends have been shifted with 20 MGI units [-] for plotting purposes.

The accurate and robust determination of the nucleation onset using the BVI approach makes it a suitable tool to be used for example in combination with the adaptive supersaturation (Woo et al., 2009) or direct nucleation control (DNC) approach (Abu Bakar M.R. et al., 2009). In the context of the DNC framework for example, by detecting the formed nuclei as soon as possible, the time required to re-dissolve the nuclei (heat-up or solvent addition phase) is minimized.

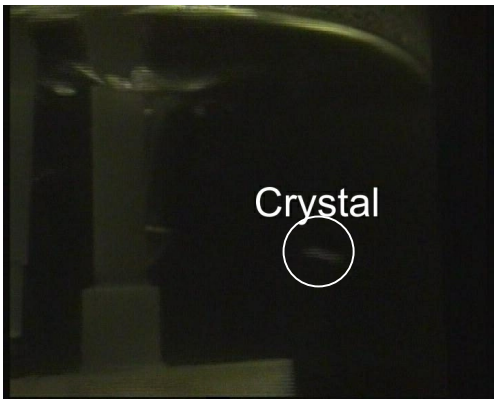

Figure 17. The crystal corresponding to the peaks in the MGI trends at 124.56 minutes.

5. Conclusions

In this work the proof of concept for the newly proposed bulk video monitoring (BVI) approach is presented. It was shown that BVI has comparable performance in detecting the nucleation onset to the FBRM and UV/Vis probes, in the case of suspension crystallization of caffeine but can provide significantly earlier detection of the apparent nucleation in the case of crystallization from melt of palm oil, where the size of the particles forming is below the detection limit of FBRM. The BVI approach is proposed as a complementary approach to the existing process analytical monitoring tools. It can be implemented as an external sensor providing significantly lower sensitivity to mixing conditions than other probes based on local measurements. Furthermore, the contamination related problems are circumvented. The advantage of the BVI approach is that it does not require high speed video camera or advanced illumination technologies such as laser or xenon flash, and is easily implementable in industrial environments.

Acknowledgements

The authors would like to acknowledge the help provided by E. Aamir, A. N. Saleemi and Dr. K. Patchigolla during the experimental work carried out at the Chemical Engineering department, Loughborough University, U.K. Elina Hishamuddin from the Malaysian Palm Oil Board is gratefully acknowledged for providing the palm oil for the experiments. The second author acknowledges the financial support provided by the Engineering and Physical Sciences Research Council (EPSRC), U.K., (grant EP/E022294/1).

References

Abu Bakar M.R., Nagy Z. K. , Saleemi A. N. , Rielly C.D., (2009). The Impact of Direct Nucleation Control on Size Distribution in Pharmaceutical Crystallization Process. Crystal Growth & Design, 9(3), 1378-1384, 2009.

Billeter, J., Neuhold, Y. M., Simon, L., Puxty, G., Hungerbuhler, K., (2008). Uncertainties and Error Propagation in Kinetic Hard-Modelling of Spectroscopic Data. Chemometrics and Intelligent Laboratory Systems, 93, 120-131.

Bothe, H., Cammenga, H. K., (1980). Composition, Properties, Stability and Thermal Dehydration of Crystalline Caffeine Hydrate. Thermochimica Acta, 40, 29-39.

Braatz, R. D., (2002). Advanced Control of Crystallization Processes. Annual Reviews in Control, 26, 87-89.

Bustamante, P., Navarro, J., Romero, S., Escalera, B., (2002). Thermodynamic Origin of the Solubility Profile of Drugs Showing One or Two Maxima against the Polarity of Aqueous and Nonaqueous Mixtures: Niflumic Acid and Caffeine. Journal of Pharmaceutical Sciences, 91, 874-883.

Calderon De Anda, J., Wang, X. Z., Lai, X., Roberts, K. J., (2005). Classifying Organic Crystals Via in-Process Image Analysis and the Use of Monitoring Charts to Follow Polymorphic and Morphological Changes. Journal of Process Control, 15, 785-797.

De Anda, J. C., Wang, X. Z., Lai, X., Roberts, K. J., Jennings, K. H., Wilkinson, M. J., Watson, D., Roberts, D., (2005). Real-Time Product Morphology Monitoring in Crystallization Using Imaging Technique. AIChE Journal, 51, 1406-1414.

Eggers, J., Kempkes, M., Mazzotti, M., (2009). Measurement of Size and Shape Distributions of Particles through Image Analysis. Chemical Engineering Science, In Press, Corrected Proof.

Fujiwara, M., Chow, P. S., Ma, D. L., Braatz, R. D., (2002). Paracetamol Crystallization Using Laser Backscattering and Atr-Ftir Spectroscopy: Metastability, Agglomeration, and Control. Crystal Growth & Design, 2, 363-370.

Gurbuz, H., Ozdemir, B., (2003). Experimental Determination of the Metastable Zone Width of Borax Decahydrate by Ultrasonic Velocity Measurement. Journal of Crystal Growth, 252, 343-349.

Joung, O. J., Kim, Y. H., Fukui, K., (2005). Determination of Metastable Zone Width in Cooling Crystallization with a Quartz Crystal Sensor. Sensors and Actuators B-Chemical, 105, 464-472.

Kempkes, M., Eggers, J., Mazzotti, M., (2008). Measurement of Particle Size and Shape by Fbrm and in Situ Microscopy. Chemical Engineering Science, 63, 4656-4675.

Kumar, F. J., Moorthy, S. G., Jayaraman, D., Subramanian, C., (1996). Estimation of Metastable Zone Width, Interfacial Energy and Growth Rates of Ktiopo4 Crystallizing from K6p4o13 Flux by Hot Stage Microscopy. Journal of Crystal Growth, 160, 129-135.
Larsen, P. A., Rawlings, J. B., Ferrier, N. J., (2007). Model-Based Object Recognition to Measure Crystal Size and Shape Distributions from in Situ Video Images. Chemical Engineering Science, 62, 1430-1441.
Li, R. F., Penchev, R., Ramachandran, V., Roberts, K. J., Wang, X. Z., Tweedie, R. J., Prior, A., Gerritsen, J. W., Hugen, F. M., (2008). Particle Shape Characterisation Via Image Analysis: From Laboratory Studies to in-Process Measurements Using an in Situ Particle Viewer System. Organic Process Research & Development, 12, 837-849.
Loffelmann, M., Mersmann, A., (2002). How to Measure Supersaturation? Chemical Engineering Science, 57, 4301-4310.
Lyczko, N., Espitalier, F., Louisnard, O., Schwartzentruber, J., (2002). Effect of Ultrasound on the Induction Time and the Metastable Zone Widths of Potassium Sulphate. Chemical Engineering Journal, 86, 233-241.
Marciniak, B., (2002a). Density and Ultrasonic Velocity of Undersaturated and Supersaturated Solutions of Fluoranthene in Trichloroethylene, and Study of Their Metastable Zone Width. Journal of Crystal Growth, 236, 347-356.
Marciniak, B., (2002b). Density and Ultrasonic Velocity of Undersaturated and Supersaturated Solutions of Fluoranthene in Trichloroethylene, and Study of Their Metastable Zone Width. Journal of Crystal Growth, 236, 347-356.
Nagy, Z. K., Chew, J. W., Fujiwara, M., Braatz, R. D., (2008). Comparative Performance of Concentration and Temperature Controlled Batch Crystallizations. Journal of Process Control, 18, 399-407.
Nagy, Z. K., Gillon, A. L., Steele, G., Makwana, N., Rielly, C. D., Using Process Analytical Technology for in Situ Monitoring of the Polymorphic Transformation of Organic Compounds, In *8th International IFAC Symposium on Dynamics and Control of Process Systems*, Cancun, Mexico, 6-8 June 2007, 2007.
O'Grady, D., Barrett, M., Casey, E., Glennon, B., (2007). The Effect of Mixing on the Metastable Zone Width and Nucleation Kinetics in the Anti-Solvent Crystallization of Benzoic Acid. Chemical Engineering Research & Design, 85, 945-952.

Parsons, A. R., Black, S. N., Colling, R., (2003). Automated Measurement of Metastable Zones for Pharmaceutical Compounds. Chemical Engineering Research & Design, 81, 700-704.
Pollanen, K., Hakkinen, A., Reinikainen, S. P., Rantanen, J., Minkkinen, P., (2006). Dynamic Pca-Based Mspc Charts for Nucleation Prediction in Batch Cooling Crystallization Processes. Chemometrics and Intelligent Laboratory Systems, 84, 126-133.
Qu, H. Y., Louhi-Kultanen, M., Kallas, J., (2006). In-Line Image Analysis on the Effects of Additives in Batch Cooling Crystallization. Journal of Crystal Growth, 289, 286-294.
Sohnel, O., Mullin, J. W., (1988). The Role of Time in Metastable Zone Width Determinations. Chemical Engineering Research & Design, 66, 537-540.
Woo, X. Y., Nagy, Z. K., Tan, R. B. H., Braatz, R. D., (2009). Adaptive Concentration Control of Cooling and Antisolvent Crystallization with Laser Backscattering Measurement. Crystal Growth & Design, 9, 182-191.